Protein kinase PKR mutants resistant to the poxvirus pseudosubstrate K3L protein

Eun Joo Seo[a], Furong Liu[a], Makiko Kawagishi-Kobayashi[a], Tekly L. Ung[a], Chune Cao[a], Arvin C. Dar[b,c], Frank Sicheri[b,c], and Thomas E. Dever[a,1]

[a]Laboratory of Gene Regulation and Development, Eunice Kennedy Shriver National Institute of Child Health and Human Development, National Institutes of Health, Bethesda, MD 20892; [b]Program in Systems Biology, Samuel Lunenfeld Research Institute, Mount Sinai Hospital, Toronto, ON, Canada M5G 1X5; and [c]Department of Molecular Genetics, University of Toronto, Toronto, ON, Canada M5S 1A8

Edited by Bernard Moss, National Institutes of Health, Bethesda, MD, and approved September 23, 2008 (received for review June 10, 2008)

As part of the mammalian cell innate immune response, the double-stranded RNA activated protein kinase PKR phosphorylates the translation initiation factor eIF2α to inhibit protein synthesis and thus block viral replication. Poxviruses including vaccinia and smallpox viruses express PKR inhibitors such as the vaccinia virus K3L protein that resembles the N-terminal substrate-targeting domain of eIF2α. Whereas high-level expression of human PKR was toxic in yeast, this growth inhibition was suppressed by coexpression of the K3L protein. We used this yeast assay to screen for PKR mutants that are resistant to K3L inhibition, and we identified 12 mutations mapping to the C-terminal lobe of the PKR kinase domain. The PKR mutations specifically conferred resistance to the K3L protein both in yeast and in vitro. Consistently, the PKR-D486V mutation led to nearly a 15-fold decrease in K3L binding affinity yet did not impair eIF2α phosphorylation. Our results support the identification of the eIF2α-binding site on an extensive face of the C-terminal lobe of the kinase domain, and they indicate that subtle changes to the PKR kinase domain can drastically impact pseudosubstrate inhibition while leaving substrate phosphorylation intact. We propose that these paradoxical effects of the PKR mutations on pseudosubstrate vs. substrate interactions reflect differences between the rigid K3L protein and the plastic nature of eIF2α around the Ser-51 phosphorylation site.

eIF2 | translational control

The interplay of viruses and mammalian cells represents an arms race of defense mechanisms and counter measures. Viral infection triggers the innate immune response, including activation of the double-stranded RNA (dsRNA)-activated protein kinase PKR. Consisting of an N-terminal dsRNA-binding domain (dsRBD) and a C-terminal kinase domain (KD), PKR is activated by dsRNA molecules generated during viral replication and gene expression. Once activated, PKR is competent to bind and phosphorylate its substrate, the α subunit of translation initiation factor eIF2 on Ser-51. The eIF2 is a GTP-binding protein that is responsible for binding the Met-tRNA$_i^{Met}$ to the small ribosomal subunit. Phosphorylation of eIF2α converts eIF2 into an inhibitor of its guanine nucleotide exchange factor eIF2B and thereby down-regulates protein synthesis. Because viral protein synthesis depends on the host cell's machinery, PKR inhibition of cellular protein synthesis will block viral mRNA translation as well. To overcome this host defense mechanism, most viruses express inhibitors of PKR.

Among the viral inhibitors of PKR are the adenoviral RNA VA-I and dsRNA-binding proteins such as the vaccinia virus E3L protein, cytomegalovirus TRS-1 and IRS-1 proteins, and reovirus σ3 (1–3). Another family of PKR inhibitors includes viral psueudosubstrates. The vaccinia virus K3L protein and the related myxoma virus M156R protein resemble the N-terminal OB-fold domain of eIF2α (4, 5) (Fig. 1*A*). Although the M156R protein appears to be a PKR substrate, the K3L protein binds to PKR and blocks PKR autophosphorylation and eIF2α phosphorylation both in vivo (6) and in vitro (4, 7). The 88-residue vaccinia virus K3L protein shares 28% amino acid sequence identity to the N terminus of eIF2α. The structures of the K3L protein and eIF2α are strikingly similar, with the greatest differences localized to the helix insert regions (Fig. 1*A*), which includes the Ser-51 phosphorylation site in eIF2α. The K3L protein directly interacts with the kinase domain of PKR, as revealed by yeast 2-hybrid and in vitro interaction assays (4, 8–11). Because the K3L protein and eIF2α were found to compete for binding to PKR (11), it is thought that they bind to the kinase by a common mechanism.

In the structure of the PKR KD bound to eIF2α, the PKR KD resembles typical protein kinases with a smaller N-terminal lobe involved in ATP binding and a larger C-terminal lobe that mediates substrate interactions (12). Dimerization of the PKR KD in a back-to-back orientation with dimer contacts restricted to the N-terminal lobe enables each protomer to engage a molecule of eIF2α. The concave surface of the eIF2α OB-fold domain docks on helix αG in the C-terminal lobe, and this positions the helix insert region and Ser-51 residue in eIF2α in the vicinity of the PKR active site in the cleft between the 2 lobes of the KD (see Fig. 1*A*). Mutational analyses demonstrated that KD dimerization and autophosphorylation on Thr-446 are critical for eIF2α phosphorylation and for binding the K3L protein (9). In addition, mutations that disrupt PKR helix αG specifically impair eIF2α phosphorylation but not kinase autophosphorylation or phosphorylation of nonspecific substrates (9). Taken together, the structural and biochemical studies reveal an eIF2α-binding site on PKR commonly engaged by K3L that extends from helix αG to the kinase active site cleft. Given this common binding site, we reasoned that PKR might recognize differences in the helix insert regions to distinguish between its authentic substrate and a pseudosubstrate inhibitor.

Further insights into the molecular mechanism of PKR recognition of eIF2α and regulation of the kinase by the K3L protein have been provided by studies in the yeast *Saccharomyces cerevisiae*. High-level expression of human PKR is toxic in yeast because of phosphorylation of eIF2α and the attendant inhibition of translation initiation (13, 14). Substitution of Ser-51 in eIF2α by Ala suppresses PKR toxicity as do mutations that block kinase activity (9, 14, 15). Coexpression of the vaccinia virus K3L protein or the related swinepox virus C8L protein suppresses PKR toxicity in yeast (16, 17). Consistent with the notion that the K3L protein is a PKR pseudosubstrate inhibitor, mutations targeting residues in the K3L OB-fold domain that are conserved in eIF2α impaired K3L inhibition of PKR both in yeast (17) and in vitro (4). Moreover, a mutation (H47R) that increased the amino acid sequence identity between K3L and eIF2α in the vicinity of the Ser-51 phosphorylation site enhanced K3L inhibition of PKR in yeast (17).

Author contributions: E.J.S., F.L., M.K.-K., F.S., and T.E.D. designed research; E.J.S., F.L., M.K.-K., T.L.U., C.C., and A.C.D. performed research; E.J.S., F.L., M.K.-K., A.C.D., F.S., and T.E.D. analyzed data; and E.J.S., F.S., and T.E.D. wrote the paper.

The authors declare no conflict of interest.

This article is a PNAS Direct Submission.

[1]To whom correspondence should be addressed. E-mail: tdever@nih.gov.

This article contains supporting information online at www.pnas.org/cgi/content/full/0805524105/DCSupplemental.

© 2008 by The National Academy of Sciences of the USA

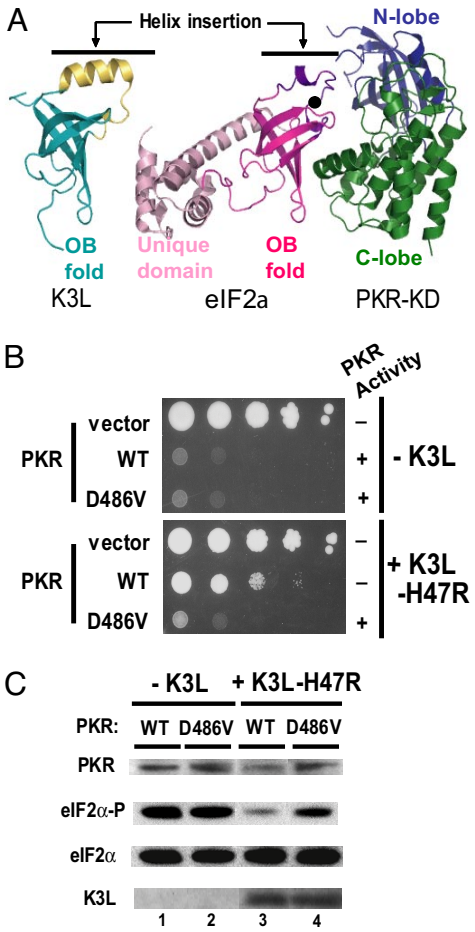

Fig. 1. Isolation of PKR mutants resistant to inhibition by the vaccinia virus K3L protein. (*A*) Ribbons representation of K3L [Protein Data Bank (PDB) ID code 1LUZ] and PKR-eIF2α complex. The PKR-eIF2α complex was generated by substituting the structure of free eIF2α (PDB ID code 1Q46), in which the structure of the helix insert region is resolved, in place of eIF2α in the PKR-eIF2α complex structure (PDB ID code 2A1A). The OB-fold domains of the PKR pseudosubstrate K3L (cyan) and authentic substrate eIF2α (red) are aligned and their helix insert regions are colored yellow (K3L) and purple (eIF2α). PKR N-lobe is colored blue; C-lobe is green; and Ser-51 phosphorylation site in eIF2α is denoted by the black circle. (*B*) Coexpression of K3L-H47R suppresses toxicity associated with expression of PKR, but not PKR-D486V, in yeast. Plasmids expressing PKR or PKR-D486V under the control of the yeast *GAL-CYC1* hybrid promoter or the empty vector pRS316 were introduced into the isogenic yeast strains J673 and J674 carrying an integrated *LEU2* vector or *GAL-CYC1-K3L-H47R* construct, respectively. The indicated yeast transformants were grown to saturation, and 5 μL of serial dilutions (of OD_{600} = 1.0, 0.1, 0.01, 0.001, and 0.0001) were spotted on SCGal-Ura medium (synthetic complete medium containing 2% galactose and lacking uracil) and incubated 3 days at 30°C. (*C*) Immunoblot analysis of PKR and K3L-H47R expression and eIF2α phosphorylation. WCEs were prepared from the yeast transformants described in *B*, as indicated. WCEs were subjected to SDS/PAGE followed by immunoblot analysis using monoclonal antibodies directed against PKR, polyclonal antiserum directed against K3L, or phosphospecific antibodies against Ser-51 in eIF2α. The eIF2α membrane was then stripped and probed using polyclonal antiserum against yeast eIF2α.

To gain further insights into how the K3L protein inhibits PKR, and to determine whether PKR can distinguish its substrate eIF2α from pseudosubstrate inhibitors, we used a genetic screen to identify PKR mutants that are resistant to inhibition by the K3L protein. Surprisingly, the mutations clustered near helix αG, a region thought to interact with K3L and eIF2α in a like manner. We propose that subtle alterations to the substrate-binding site on PKR can differentially affect substrate and pseudosubstrate interactions, perhaps reflecting differences in the adaptability of the K3L pseudosubstrate and eIF2α to perturbations that alter the spacing between the helix αG docking site and the kinase active site cleft.

Results

Screen to Identify PKR Mutants Resistant to Inhibition by the Vaccinia Virus K3L Protein. Previously, we showed that high-level expression of human PKR under the control of a yeast galactose-inducible promoter was toxic in yeast, and that this toxicity was suppressed by coexpression of the vaccinia virus K3L protein. In addition, we identified the K3L-H47R mutant as a more potent inhibitor of PKR (16, 17). To facilitate screening for PKR mutants resistant to K3L inhibition, the DNA fragment encoding the galactose-inducible *GAL-CYC1* promoter and the K3L-H47R ORF was subcloned to a yeast-integrating vector. We chose to use the robust K3L-H47R mutant for this screen, because it provided a larger window to observe restoration of PKR activity in yeast. The resulting construct and the related empty vector control were directed to integrate at the *leu2* locus of a *gcn2*Δ strain creating the *GAL-CYC1-K3L-H47R* strain J674 and the vector control strain J673. As expected, Western blot analyses of extracts from cells grown on galactose medium revealed robust expression of K3L-H47R in J674 but not in J673 (Fig. 1*C*, bottom). The expression of human PKR under the control of a galactose-inducible promoter was lethal in strain J673 (Fig. 1*B Lower*); however, this toxicity was substantially suppressed in strain J674 that expresses the K3L-H47R protein (Fig. 1*B*, fifth row). Consistent with these growth phenotypes, expression of the K3L-H47R protein diminished eIF2α phosphorylation on Ser-51 (Fig. 1*C*, second row, lane 3 vs. lane 1).

We used the K3L-H47R strain to screen for PKR mutants resistant to pseudosubstrate inhibition. The *GAL-CYC1-PKR* expression vector p1419 was subjected to random mutagenesis by passage through the bacterial mutator strain XL1-red, and the resultant PKR mutant library was introduced into the *GAL-CYC1-K3L-H47R* strain J674. Transformants were replica-plated to medium containing galactose to induce both K3L-H47R and PKR expression, and colonies that grew slower than controls expressing WT PKR were selected for further analysis. From a screen of $\approx$4,000 yeast transformants, 99 colonies grew slower than the WT control, with 38 of this latter set showing a strong slow-growth phenotype. Sequence analysis of the resistant clones revealed that several of the mutants were isolated more than once, and that 28 contained multiple mutations. Individual point mutations were introduced into the WT PKR expression construct and tested for resistance to K3L inhibition. Finally, 12 single amino acid changes in the PKR kinase domain were identified as conferring resistance to inhibition by K3L-H47R in the yeast assay: E375V, I378T, R382I, I405M, S448G, M455V, A473T, E480D, D486V, T491S, S504L, and E524V [see Fig. 2*A Left* and supporting information (SI) Fig. S1].

As shown in Fig. 1*B*, the representative PKR-D486V mutant strongly inhibited the growth of yeast both lacking and expressing K3L-H47R. Consistently, expression of PKR-D486V led to high levels of eIF2α phosphorylation on Ser-51 both in the absence and presence of K3L-H47R coexpression (Fig. 1*C*, lanes 2 and 4). Western blot analyses of crude extracts from yeast expressing the other K3L-H47R-resistant mutants of PKR revealed similar high levels of Ser-51 phosphorylation (Fig. S2), indicating that the PKR mutations inhibit yeast cell growth by restoring eIF2α phosphorylation activity in the presence of K3L-H47R.

PKR Mutants Are Specifically Resistant to K3L Inhibition. The growth inhibition observed in the K3L-H47R strains expressing the PKR mutants could be due to enhanced eIF2α phosphorylation, as shown in Fig. 1*C*, or it could possibly be due to promiscuous phosphorylation of other substrates by the mutant forms of PKR.

BIOCHEMISTRY

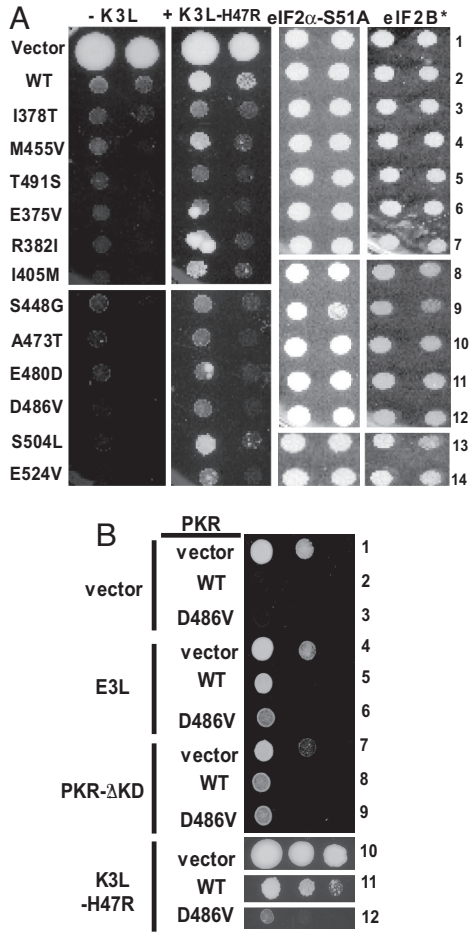

Fig. 2. PKR mutations specifically confer resistance to K3L inhibition. (*A*) PKR mutant toxicity is suppressed in eIF2α-S51A and eIF2Bα mutant strains. Plasmids expressing WT or the indicated PKR mutants were introduced into strains J673 (-K3L), J674 (+K3L-H47R), J82 (eIF2α-S51A), and H17 (eIF2B*). Transformants were grown and serial dilutions (of OD_{600} = 1.0 and 0.1) were spotted as described in Fig. 1*B*, except that transformants of strain H17 were grown on medium containing 10%, instead of 2%, galactose. [The complete spotting assay (of OD_{600} = 1.0, 0.1, 0.01, 0.001, and 0.0001) is presented in Fig. S1.] (*B*) PKR mutants are specifically resistant to inhibition by the K3L protein. Plasmids expressing PKR or PKR-D486V, or the empty vector pRS316, were introduced into the isogenic yeast strains J673 (vector), J659 (E3L), J662 (PKR^{1-258} = PKR-ΔKD), and J674 (K3L-H47R). Transformants were grown and serial dilutions (of OD_{600} = 1.0, 0.1, and 0.01) were spotted as described in Fig. 1*B*.

To test whether the PKR mutations relaxed the kinase specificity and conferred toxicity in yeast because of phosphorylation of proteins other than eIF2α, we expressed the PKR mutants in the strain J82 expressing nonphosphorylatable eIF2α-S51A. As shown in Fig. 2*A*, the toxic affects associated with high-level expression of WT PKR were suppressed in the eIF2α-S51A strain (compare rows 1 and 2 in the first and third sections). Likewise, the toxic affects of all of the PKR mutants except PKR-S448G were suppressed in the eIF2α-S51A strain (Fig. 2*A Right Center*, and more apparent in Fig. S1, row 9). Thus, the majority of the PKR mutants are toxic in yeast expressing K3L-H47R because of enhanced eIF2α phosphorylation.

Whereas expression of WT PKR is lethal in yeast expressing WT eIF2B, high-level expression of WT PKR causes a slow-growth phenotype in a desensitized yeast strain expressing eIF2Bα-E44D (*gcn3-102* mutant allele in strain H17; see Fig. 2*A Left* and *Right*, row 2). If the PKR mutations conferred resistance to K3L-H47R inhibition by hyperactivating the kinase, then these mutants should be more toxic than WT PKR in the eIF2Bα mutant strain. In contrast, expression of the PKR mutants, except PKR-S448G, conferred the same slow-growth phenotype observed with WT PKR (Fig. 2*A Right*, and more apparent in Fig. S1, row 9). We conclude that the K3L-H47R-resistant PKR mutants are not simply hyperactive kinases. Moreover, the lack of an additional growth defect when expressing the PKR mutants in the eIF2Bα mutant strain is consistent with the results of Western analyses that showed that the PKR mutants were not overexpressed relative to WT PKR (Fig. S3, and data not shown). Thus, these results indicate that the mutations restore PKR toxicity in yeast by specifically impairing K3L-H47R inhibition of kinase activity. In contrast, the S448G mutation likely loosens PKR substrate specificity resulting in promiscuous phosphorylation of other proteins and growth inhibition.

To examine the specificity of the PKR mutations in conferring resistance to K3L-H47R vs. other inhibitors, we tested the inhibition of PKR by the vaccinia virus dsRNA-binding E3L protein and by the dominant-negative N-terminal portion of PKR. For these experiments, we focused on the PKR-D486V mutant; however, similar results were obtained for all of the PKR mutants. Coexpression of the vaccinia virus E3L protein or the N-terminal portion of PKR (residues 1–258 containing the dsRNA-binding domain and lacking the kinase domain, PKR-ΔKD) partially suppressed the growth inhibition caused by expression of WT PKR in yeast (Fig. 2*B*, rows 2, 5, and 8). These PKR inhibitors are thought to block PKR activation through heterodimer formation mediated through the N-terminal dsRNA-binding domains in PKR. Whereas PKR-D486V was resistant to inhibition by the K3L-H47R protein, the toxic affects associated with expression of PKR-D486V in yeast, like WT PKR, was partially suppressed by coexpression of the E3L protein or PKR-ΔKD (Fig. 2*B*, rows 3, 6, and 9). In contrast, PKR-D486V was resistant to inhibition by WT K3L (Fig. S4*A*) or by the smallpox virus pseudosubstrate C3L protein (Fig. S5). Thus, we conclude that the PKR mutations specifically confer resistance to pseudosubstrate inhibition by the K3L protein.

PKR Mutations Map to the C-Terminal Lobe of the PKR Kinase Domain. The crystal structure of eIF2α bound to PKR revealed an extensive interface with the OB-fold domain of eIF2α docking on helix αG in the C-terminal lobe of PKR kinase domain (see Fig. 3*A*). Helix αG is a notable feature of eIF2α kinases in that it is 1 turn longer and 40° tilted from the canonical αG observed in all other proteins kinases studied to date (12). This distinct feature is thought to impart the eIF2α protein kinases with the unique ability to bind and phosphorylate eIF2α on Ser-51. Aside from helix αG the only other notable contact of eIF2α to PKR is directed at the *P* + 1 portion of the kinase domain activation segment. The conformation of the *P* + 1 loop of protein kinases defines their specificity for Ser/Thr (outward *P* + 1 orientation) vs. Tyr (inward orientation) hydroxyl groups by providing a platform within the active site that positions the mainchain atoms of the phosphoacceptor site. The *P* + 1 loop of PKR was notable in adopting a conformation unique from both Ser/Thr and Tyr kinases. This unusual feature likely reflects a unique constraint imposed on the eIF2α kinases required for eIF2α recognition.

When mapped on the structure of the PKR kinase domain, all 12 K3L-resistant mutations in PKR localized to the C-terminal lobe of the kinase domain (Fig. 3*A*). Interestingly, 9 of the 12 mutations cluster to the immediate vicinity of the eIF2α-binding site at the tip of helix αG and to the *P* + 1 portion of the kinase activation segment (Fig. 3*B*). The residues E375, I378 and R382 on helix αD, E480 on helix αF, D486 on the αF-αG linker and T491 on helix αG form a network of interacting residues that supports the eIF2α kinase specific orientation of helix αG. In contrast, S448 and M455 reside within the kinase domain activation segment and help to define the eIF2α specific conformation of the *P* + 1 loop subelement. Also residing in the *P* + 1 loop cluster, A473 in helix αF forms part of the hydrophobic core that backstops Met-455.

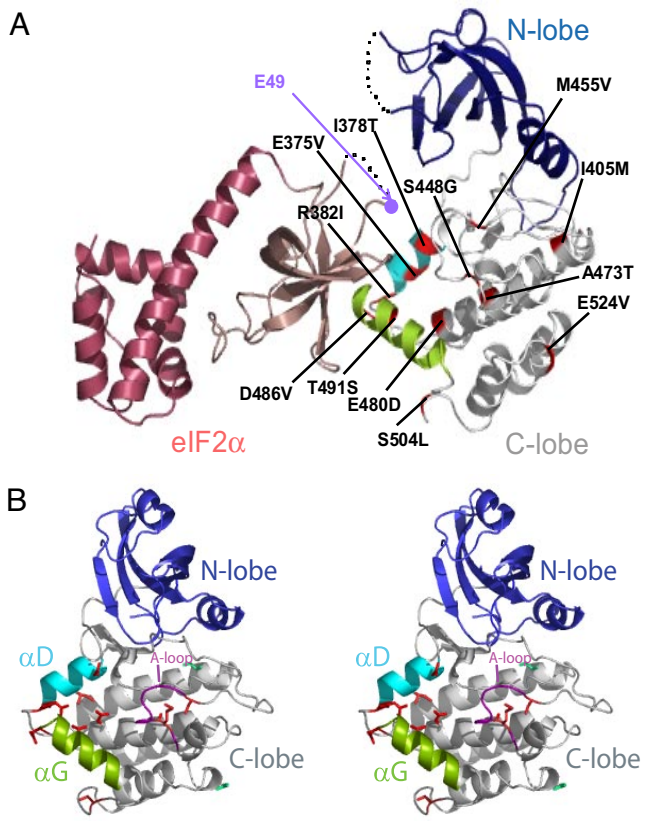

Fig. 3. K3L-resistant mutations cluster near the substrate-docking site in PKR. (*A*) Ribbons representation of the PKR-eIF2α complex (PDB code 2A1A). The OB-fold domain of eIF2α is colored dark salmon and the α-helical domain is depicted in magenta. The N- and C-lobes of the PKR kinase domain are colored blue and gray, respectively; helix αD is colored cyan and helix αG is shown in green. PKR mutations that confer resistance to K3L inhibition are labeled and shaded red. The residue E49 in eIF2α is labeled and denoted by the purple circle; residues 50–59 in eIF2α and residues 338–351 in PKR are depicted by dashed lines because of disorder and/or deletion in the structure. (*B*) Stereo image of ribbons representation of PKR mutants. PKR is shaded as described in panel A with the *P* + 1 loop colored purple. PKR mutations that confer resistance to K3L inhibition are depicted as sticks and colored red if located near αG or *P* + 1 loop or colored green if located elsewhere.

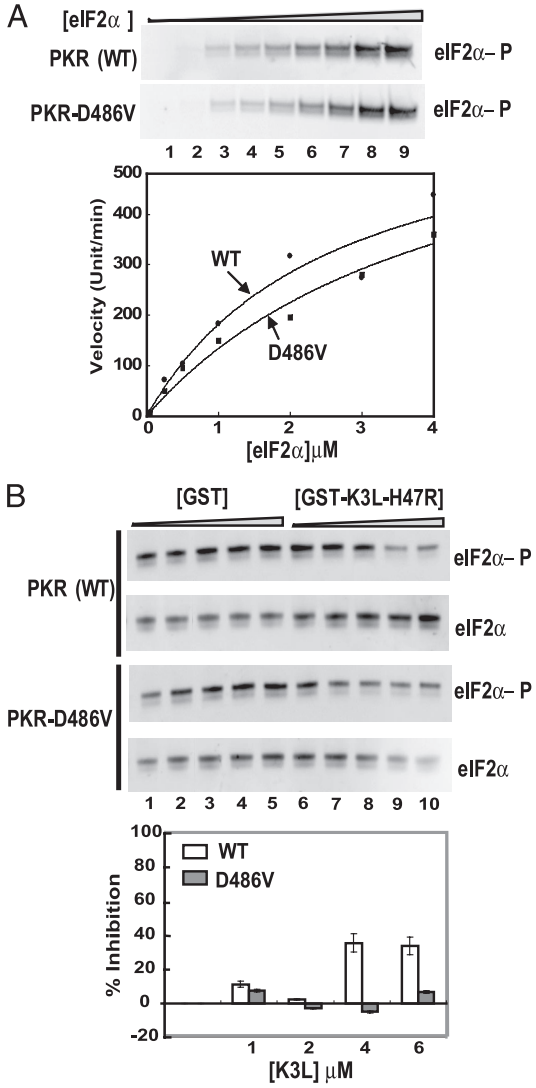

Fig. 4. PKR-D486V mutation confers resistance to inhibition by K3L in vitro. (*A*) Kinetic analysis of eIF2α phosphorylation by PKR and PKR-D486V. After overexpression in yeast, WT and the D486V mutant version of purified FLAG-His-PKR (2.5 nM) were incubated with [γ-^{33}P]ATP and various amounts [25, 50, and 250 nM, and 1, 2, 3, 4, and 5 μM] of recombinant His-tagged eIF2α (residues 1–200). (*Upper*) In vitro kinase reactions were resolved by SDS/PAGE, and subjected to autoradiography to visualize phosphorylated eIF2α (eIF2α-P). (*Lower*) The relative incorporation of phosphate into eIF2α was determined by using a PhosphorImager (Amersham). The data are expressed using arbitrary units, and the results are representative of 3 independent experiments. (*B*) Inhibition of WT PKR, but not PKR-D486V, by K3L-H47R in vitro. (*Upper*) Purified FLAG-His-PKR or FLAG-His-PKR-D486V (2.5 nM) were preincubated with various amounts of purified GST (lanes 1–5) or GST-K3L-H47R (lanes 6–10; 0.5, 1, 2, 4, or 6 μM) for 10 min at room temperature, then kinase reactions were initiated by addition of His-tagged eIF2α^{1-200} (0.2 μM) and 0.2 mM ATP. Reactions were resolved by SDS/PAGE and subjected to immunoblot analysis using phosphospecific antibodies against Ser-51 in eIF2α (first and third panel, eIF2α-P). The membranes were then stripped and probed using polyclonal antiserum against yeast eIF2α (second and fourth panel, eIF2α). (*Lower*) Relative phosphorylation of eIF2α in 3 independent experiments was determined by quantitative densitometry using ImageQuant (Amersham) software. Percentage inhibition was determined by comparing the eIF2α phosphorylation results from reactions containing GST-K3L-H47R vs. GST.

Together, the 9 aforementioned mutation sites appear well placed to influence the binding of substrate and pseudosubstrate. Because K3L and eIF2α are thought to share a common binding mode to PKR through a similar but not identical complement of interacting residues, these 9 sites of mutation in PKR may differentially affect binding of the 2 proteins by subtly changing local structure. We hypothesize that these 9 mutations perturb binding of the pseudosubstrate (K3L) to a greater extent than the authentic substrate (eIF2α).

PKR-D486V Mutation Impairs K3L Binding and Confers Resistance to K3L Inhibition of eIF2α Phosphorylation in Vitro. To corroborate our in vivo results, we performed a detailed analysis of PKR mutant function in vitro. Purified WT PKR and PKR-D486V were incubated with recombinant eIF2α and [γ-^{33}P]ATP and tested for phosphorylation of eIF2α using in vitro kinase assays. As shown in Fig. 4*A*, both WT PKR and PKR-D486V readily phosphorylated eIF2α. Kinetic analysis of the phosphorylation reactions (Fig. 4*A Lower*) revealed similar K_m values for eIF2α phosphorylation by WT PKR (K_m = 2.7 μM) and PKR-D486V (K_m = 3.4 μM). Thus, the D486V mutation did not significantly affect the eIF2α substrate binding properties of PKR. To study the inhibition of PKR by K3L in vitro, recombinant GST or GST-K3L-H47R fusion protein was added to the in vitro kinase assays. In addition, to specifically examine eIF2α phosphorylation on Ser-51, unlabeled ATP was used in the assays and eIF2α phosphorylation was monitored by Western blot analysis by using antibodies directed against phospho-

BIOCHEMISTRY

Ser-51 on eIF2α. As shown in Fig. 4*B*, upper), addition of GST-K3L-H47R, but not GST, inhibited Ser-51 phosphorylation by WT PKR. In contrast, Ser-51 phosphorylation by the PKR-D486V mutant was not impaired by the addition of GST-K3L-H47R (Fig. 4*B*, third and fourth sections). As shown in Fig. 4*B*, lower, addition of GST-K3L-H47R resulted in an ≈40% inhibition of eIF2α phosphorylation by WT PKR. In contrast, phosphorylation of eIF2α by PKR-D486V was insensitive to inhibition by GST-K3L-H47R up to the maximum concentration of inhibitor that could be added in these assays (Fig. 4*B*, lower). Consistent with these data, PKR-D486V phosphorylation of eIF2α was likewise resistant to inhibition by a WT GST-K3L fusion protein in vitro (Fig. S4*B*).

The results of the in vitro kinase assays suggested that the D486V mutation impaired K3L binding to PKR. Because of poor solubility that limited the concentration of K3L that could be added to the in vitro kinase assays, we were unable to measure a K_i for K3L inhibition of PKR and PKR-D486V. Instead, we used surface plasmon resonance (SPR) to examine the binding of GST-PKR-KD and GST-PKR-KD-D486V fusion proteins to immobilized WT K3L. The dimeric GST-PKR-KD readily bound to the immobilized K3L (Fig. 5*A Upper*) with an observed K_d of 3.7 μM (Fig. 5*B*). Under the conditions of this SPR experiment, GST-PKR-KD-D486V displayed minimal binding to the K3L protein (Fig. 5*A Lower*), and the K_d for binding was elevated minimally 14-fold (K_d = 53.0 μM, Fig. 5*B*). These results, which are consistent with the lack of inhibition of PKR-D486V by GST-K3L or GST-K3L-H47R in the in vitro kinase assays, indicate that the D486V mutation confers PKR resistance to K3L inhibition by selectively weakening the binding of the pseudosubstrate to the kinase.

Discussion

The structures of K3L and eIF2α are strikingly similar, with the only major differences residing in the helix insert region (Fig. 1*A*). The helix insert region in eIF2α consists of 2 short 3/10 helices separated by a linker containing the phospho-accepting Ser-51 residue (Fig. 1*A*) (18). Structural analyses of free eIF2α indicate that, although the helix insert can adopt a precise ordered conformation, it is likely to be inherently flexible in nature [as reflected by high relative B-factors (18, 19)]. This is consistent with the observation that the helix insert region of eIF2α was dynamically disordered in the PKR-eIF2α complex structure (12). Moreover, in docking the structure of free eIF2α onto the PKR-eIF2α complex it is apparent that Ser-51 must move ≈17 Å to access the PKR active site to accept phosphate. Taken together, these findings indicate that a flexible helix insert region in eIF2α is likely to be an important determinant of its ability to be phosphorylated by PKR. In contrast, the helix insert region of K3L is comprised by a 4-turn α-helix and a 3/10 helix, which appears to be rigid as indicated by its well-ordered structure with low relative B-factors (4). Inability to undergo conformation change may account in part for why K3L unlike eIF2α is not a substrate.

Given that eIF2α and K3L share an overlapping binding site on PKR, it was not unexpected that mutations in PKR that affect K3L binding map to the region of PKR extending from helix αG to the P + 1 loop in the catalytic cleft. However, because the structural differences between eIF2α and K3L are localized to the helix insert region, and this element of eIF2α docks into the kinase active site, we reasoned that PKR mutations conferring resistance to K3L (but not affecting eIF2α binding) would be biased away from helix αG and instead localize more toward the catalytic cleft (the P + 1 loop for example). Indeed, we showed that mutation of Thr-487 at the tip of helix αG blocked eIF2α phosphorylation (9). Therefore, we were surprised that the majority of the K3L-resistant mutations in PKR clustered near helix αG.

So why is it that we identified so many mutations in and around helix αG that confer resistance to K3L and so few mutations in the vicinity of the kinase active site? One possibility is that mutations in the kinase active site region that perturb K3L binding have a greater probability of perturbing protein kinase catalytic function. Because the yeast genetic screen demanded both impaired K3L inhibition and robust eIF2α kinase activity, mutations in the active site might have been excluded because of negative effects on eIF2α phosphorylation. This counterselection against active-site mutations limited mutations to the helix αG region of PKR, the only other region that makes prominent contacts with substrate or pseudosubstrate.

So how do mutations in the helix αG region of PKR confer resistance to K3L inhibition? Because the toxic phenotypes of the

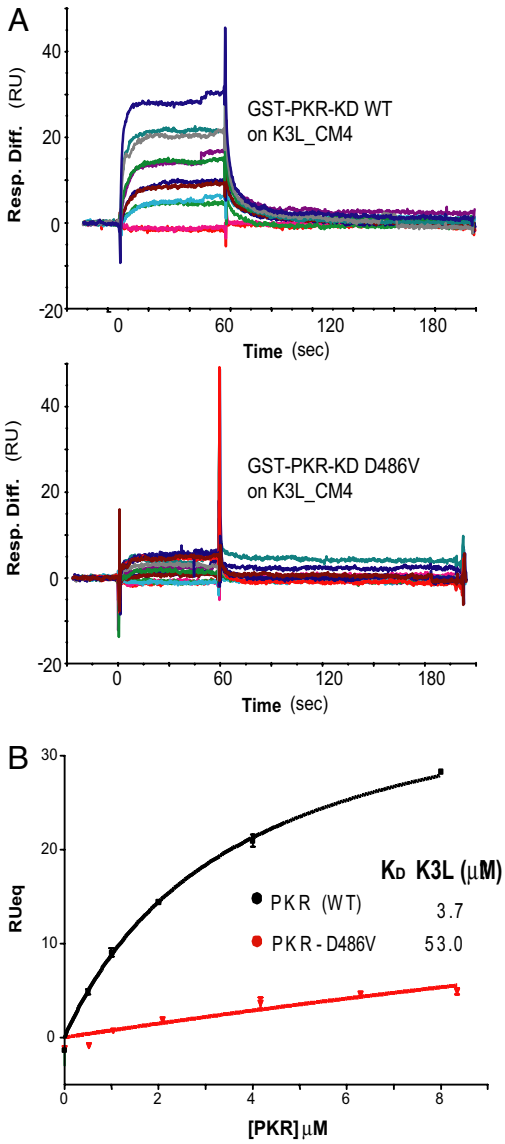

Fig. 5. SPR analysis reveals D486V mutation impairs PKR binding to K3L protein. (*A*) Sensorgrams of WT (*Upper*) or D486V mutant (*Lower*) version of GST fused PKR-KD binding to WT K3L. Recombinant GST-PKR-KD (PKR$^{258–551}$-Δ13-H412N-C551A) was applied to a K3L amine-coupled CM4 chip at 0.5, 1.0, 2.0, 4.0, 6.0, and 8.0 μM concentrations (blue, cyan, gray, pink, green, blue, green, and red curves in each sensorgram, respectively). (*B*) Analysis of equilibrium dissociation constants for binding of GST-PKR-KD and GST-PKR-KD-D486V to WT K3L. Response units at equilibrium (RUeq) from the application of GST-PKR-KD (black curve) or GST-PKR-KD-D486V (red curve) to K3L immobilized on CM4 chips are plotted as a function of protein-kinase concentration. RUeq is derived from the steady-state plateau of the association phases of the sensorgrams shown in *A*. Equilibrium dissociation constants were determined by using the analysis software BIAEVALUATION 4.0.1 (BIAcore).

PKR mutants (other than S448G) were suppressed in the eIF2α-S51A strain (Fig. 2*A*), the PKR mutations did not confer toxicity in yeast through broadened substrate recognition properties and promiscuous phosphorylation of heterologous substrates. Likewise, because the mutant forms of PKR were not more toxic than WT PKR in the eIF2Bα mutant strain (Fig. 2*A*), and WT PKR and PKR-D486V phosphorylated eIF2α with similar kinetic properties (K_m and V_{max}, Fig. 4*A*), the PKR mutations do not hyperactivate the kinase. In contrast, SPR experiments showed that the D486V mutation decreased PKR affinity for K3L by ≈14-fold (Fig. 5), indicating that the mutations specifically weakened pseudosubstrate binding to PKR.

We propose that differences in the relative flexibility of K3L and eIF2α account for the apparent specificity of the PKR helix αG mutations. The OB-fold domain of the rigid K3L protein docks on PKR helix αG, and its helix insert region likely contacts the active-site cleft to form a stable complex. Contacts with both helix αG and the active-site cleft contribute to K3L affinity for PKR, as evidenced by the fact that mutations on the surface of the K3L OB-fold domain (Y76K) and in the helix insert (V44Q) dramatically impair the ability of K3L to bind to and inhibit PKR catalytic activity (4). Like K3L, the eIF2α OB-fold domain docks on PKR helix αG positioning the helix insert region near the active site. However, in contrast to K3L, the helix insert region of eIF2α undergoes a conformational change to position the Ser-51 residue at the phospho-acceptor site in the kinase (12). Thus, we propose the flexible helix insert in eIF2α distinguishes the PKR substrate from its pseudosubstrate with a rigid helix insert. Interestingly, the identified hyperactive K3L-F36S mutant (17) readily suppressed PKR and PKR-D486V toxicity in yeast (Fig. S4*A*), and recombinant GST-K3L-F36S inhibited eIF2α phosphorylation in vitro by both PKR and PKR-D486V (Fig. S4*B*). Although remote from the region of K3L that contacts PKR, the F36S mutation is located near the beginning of strand β3 that precedes the helix insert region. Perhaps the F36S mutation alters the spacing between the OB-fold and helix insert region such that K3L can inhibit both WT PKR and the PKR-D486V mutant.

It is interesting that most of the PKR mutations conferring resistance to K3L do not lie at points of contact between PKR and eIF2α, rather the mutations appear to be slightly removed from the contact points. We propose that these mutations slightly alter the position of the eIF2α/K3L contact sites. For example, the mutations in helix αF, which lies behind and buttresses helix αG, are likely to alter the position of helix αG. Slightly moving helix αG may significantly impair binding of K3L, because the helix insert region will no longer properly contact the PKR active site. In contrast, slight repositioning of helix αG may not affect eIF2α phosphorylation, because the flexible helix insert region can compensate for the altered docking and still insert the Ser-51 residue into the kinase active site. Further insights into the mechanism of action of the PKR suppressor mutations and the structural differences underlying the alternate functions of K3L and eIF2α await structural analysis of a PKR-K3L complex, and comparison with the existing complex between PKR and eIF2α.

Materials and Methods

Yeast Strains. Strains H17 (*MATα gcn3-102 leu2-3 leu2-112 ura3-52*) (20) and J82 (*MATa ura3-52 leu2-3 leu2-112 trp1-63 gcn2Δ sui2Δ* p[*SUI2-S51A*, *LEU2*]) (21) have been described. Strains J673 (*MATα ura3-52 leu2-3 leu2-112 trp1-63 gcn2Δ sui2Δ <LEU2>*), J674 (*MATα ura3-52 leu2-3 leu2-112 trp1-63 gcn2Δ sui2Δ <GAL-CYC1-K3L-H47R, LEU2>*), J659 (*MATα ura3-52 leu2-3 leu2-112 trp1-63 gcn2Δ sui2Δ <GAL-CYC1-E3L, LEU2>*), J662 (*MATα ura3-52 leu2-3 leu2-112 trp1-63 gcn2Δ sui2Δ <GAL-CYC1-PKR$^{1-258}$, LEU2>*) and J731 (*MATα ura3-52 leu2-3 leu2-112 trp1-63 gcn2Δ sui2Δ <GAL-CYC1-K3L, LEU2>*) were constructed by integrating the *LEU2* vector pRS305 or its derivatives containing galactose-inducible alleles of vaccinia virus K3L-H47R, WT K3L, variola virus E3L or PKR$^{1-258}$, as indicated, at the *leu2* locus of the strain H2557.

Experimental Conditions. Immunoblot analyses of protein expression and eIF2α phosphorylation in yeast were performed as described in ref. 9. Yeast transformants were grown in SD medium to log phase and then transferred to SGal medium (2% galactose) for 12–16 h to induce PKR and K3L expression. Whole-cell extracts (WCEs) (≈2–5 μg) were resolved by SDS/PAGE and subjected to immunoblot analysis using antibodies specific for phospho-Ser-51 on eIF2α (BioSource International), polyclonal antiyeast eIF2α antiserum, monoclonal antibodies against an N-terminal epitope in human PKR (lot71/10, Ribogene), or polyclonal K3L antiserum. Additional methods are provided in *SI Text*.

ACKNOWLEDGMENTS. We thank members of the laboratories of T.E.D., F.S., and Alan Hinnebusch for advice and discussions and Alan Hinnebusch for comments on the manuscript. We thank Eileen Chou for assistance with the genetic characterization of the PKR mutants and Craig Cameron (Pennsylvania State University) for the pGEX-3X-K3L plasmid. This work was supported in part by the Intramural Research Program of the National Institute for Child Health and Human Development, National Institutes of Health (T.E.D.) and by grants from the National Cancer Institute of Canada (to F.S.). A.C.D. was a recipient of a Canadian Graduate Scholarship from the Canadian Institutes for Health Research. F.S. is a recipient of a National Cancer Institute of Canada Scientist award.

1. Child SJ, Hakki M, De Niro KL, Geballe AP (2004) Evasion of cellular antiviral responses by human cytomegalovirus TRS1 and IRS1. *J Virol* 78:197–205.
2. Gale M, Jr, Katze MG (1998) Molecular mechanisms of interferon resistance mediated by viral-directed inhibition of PKR, the interferon-induced protein kinase. *Pharmacol Ther* 78:29–46.
3. Mohr IJ, Pe'ery T, Mathews MB (2007) in *Translational Control in Biology and Medicine*, eds Mathews MB, Sonenberg N, Hershey JWB (Cold Spring Harbor Lab Press, Cold Spring Harbor, MS), pp 545–599.
4. Dar AC, Sicheri F (2002) X-ray crystal structure and functional analysis of vaccinia virus K3L reveals molecular determinants for PKR subversion and substrate recognition. *Mol Cell* 10:295–305.
5. Ramelot TA, *et al.* (2002) Myxoma virus immunomodulatory protein M156R is a structural mimic of eukaryotic translation initiation factor eIF2α. *J Mol Biol* 322:943–954.
6. Davies MV, Elroy-Stein O, Jagus R, Moss B, Kaufman RJ (1992) The vaccinia virus K3L gene product potentiates translation by inhibiting double-stranded-RNA-activated protein kinase and phosphorylation of the α subunit of eukaryotic initiation factor 2. *J Virol* 66:1943–1950.
7. Carroll K, Elroy-Stein O, Moss B, Jagus R (1993) Recombinant vaccinia virus K3L gene product prevents activation of double-stranded RNA-dependent, initiation factor 2α-specific protein kinase. *J Biol Chem* 268:12837–12842.
8. Craig AWB, Cosentino GP, Donze O, Sonenberg N (1996) The kinase insert domain of interferon-induced protein kinase PKR is required for activity but not for interaction with the pseudosubstrate K3L. *J Biol Chem* 271:24526–24533.
9. Dey M, *et al.* (2005) Mechanistic link between PKR dimerization, autophosphorylation, and eIF2α substrate recognition. *Cell* 122:901–913.
10. Gale M, Tan S-L, Wambach M, Katze MG (1996) Interaction of the interferon-induced PKR protein kinase with inhibitory proteins P58^{IPK} and vaccinia virus K3L is mediated by unique domains: Implications for kinase regulation. *Mol Cell Biol* 16:4172–4181.
11. Sharp TV, Witzel JE, Jagus R (1997) Homologous regions of the α subunit of eukaryotic translational initiation factor 2 (eIF2α) and the vaccinia virus K3L gene product interact with same domain within the dsRNA-activated protein kinase (PKR). *Eur J Biochem* 250:85–91.
12. Dar AC, Dever TE, Sicheri F (2005) Higher-order substrate recognition of eIF2α by the RNA-dependent protein kinase PKR. *Cell* 122:887–900.
13. Chong KL, *et al.* (1992) Human p68 kinase exhibits growth suppression in yeast and homology to the translational regulator GCN2. *EMBO J* 11:1553–1562.
14. Dever TE, *et al.* (1993) Mammalian eukaryotic initiation factor 2α kinases functionally substitute for GCN2 in the *GCN4* translational control mechanism of yeast. *Proc Natl Acad Sci USA* 90:4616–4620.
15. Romano PR, Green SR, Barber GN, Mathews MB, Hinnebusch AG (1995) Structural requirements for double-stranded RNA binding, dimerization, and activation of the human eIF-2α kinase DAI in *Saccharomyces cerevisiae*. *Mol Cell Biol* 15:365–378.
16. Kawagishi-Kobayashi M, Cao C, Lu J, Ozato K, Dever TE (2000) Pseudosubstrate inhibition of protein kinase PKR by swine pox virus C8L gene product. *Virology* 276:424–434.
17. Kawagishi-Kobayashi M, Silverman JB, Ung TL, Dever TE (1997) Regulation of the protein kinase PKR by the vaccinia virus pseudosubstrate inhibitor K3L depends on residues conserved between the K3L protein and the PKR substrate eIF2α. *Mol Cell Biol* 17:4146–4158.
18. Dhaliwal S, Hoffman DW (2003) The crystal structure of the N-terminal region of the α subunit of translation initiation factor 2 (eIF2α) from Saccharomyces cerevisiae provides a view of the loop containing serine 51, the target of the eIF2α-specific kinases. *J Mol Biol* 334:187–195.
19. Nonato MC, Widom J, Clardy J (2002) Crystal structure of the N-terminal segment of human eukaryotic translation initiation factor 2α. *J Biol Chem* 277:17057–17061.
20. Harashima S, Hannig EM, Hinnebusch AG (1987) Interactions between positive and negative regulators of *GCN4* controlling gene expression and entry into the yeast cell cycle. *Genetics* 117:409–419.
21. Ung TL, Cao C, Lu J, Ozato K, Dever TE (2001) Heterologous dimerization domains functionally substitute for the double-stranded RNA binding domains of the kinase PKR. *EMBO J* 20:3728–3737.